Code and Carrier Tracking for Spectrally Asymmetric Signals

Thomas Pany, *Universität der Bundeswehr München (UFAF),* 85577 Neubiberg, Germany

Chun Yang, *SigTem Technology, Inc.*, San Mateo, CA 94402

BIOGRAPHIES

Prof. Thomas Pany is with the Universität der Bundeswehr München (also known as UFAF) at the faculty of aerospace engineering and Institute for Space Technology and Space Applications (ISTA). He teaches satellite navigation and orbit determination. His research interests include GNSS signals (in particular for Galileo second generation), GNSS receiver design, integration with other sensors and space navigation with and without GNSS. He is developing a modular GNSS test bed for advanced navigation research. Previously he worked for IFEN GmbH and IGASPIN GmbH and is the architect of the SX3 software receiver.

Dr. Chun Yang received his Bachelor of Engineering from the Northeastern University (Shenyang, China) and the title of Docteur en Science from the Université de Paris-Sud (Orsay, France). After postdoctoral research at the University of Connecticut (Storrs, CT), he has been working on adaptive array and baseband signal processing for GNSS, radar, and communications systems and nonlinear state estimation in such applications as target tracking, integrated inertial navigation, and information fusion. Dr. Yang is the winner of 2009 IEEE NAECON Grand Challenge and the recipient of 2007 ION Samuel Burka Award.

ABSTRACT

Standard GNSS signals like binary phase shift keying (BPSK) or binary offset carrier (BOC) signals exhibit a spectrum symmetric with respect to the nominal center frequency. The corresponding signal tracking theory is well established and describes the noise performance of code and carrier tracking in terms of 1-sigma values for delay, frequency and phase lock loops (DLL, FLL or PLL) tracking errors plus the corresponding Cramér-Rao lower bounds. Recently more generalized GNSS signals have been either proposed or constructed from existing signals. Their spectrum is not symmetric anymore, which impacts code and carrier tracking. Examples for those signals are the introduction of a possible third signal component to an existing open service signal with a frequency offset, the combined coherent tracking of two legacy GNSS signals (e.g. L5+L2C) known as metasignal concept [4], or the intentional offset of the nominal frequency of a legacy signal to sharpen the correlation peak known as variable IF tracking loop (VITAL) concept [2].

Within this paper we apply the standard tracking theory for spectrally asymmetric signals. Spectral asymmetry should result in a generally increased code tracking accuracy as the spectral energy is located near to one or the other edge of the signal bandwidth yielding sharper correlation peaks. This is nicely exploited in the VITAL scheme. An implementation of the VITAL concept within a MATLAB-based software receiver demonstrates that the increased code tracking accuracy transfers also to increased positioning results for real-world GPS C/A signals. The correlation depends on the spectral asymmetry and in a sense the VITAL concept can be seen as a gradual way to include carrier accuracy into the code tracking.

A more detailed single channel analysis with two different software receiver shows, however, a discrepancy between expected accuracy gain and true accuracy gain. This could be due to a drawback of spectrally asymmetric signals, that is, code phase and carrier phase estimates become correlated and cycle slips or carrier tracking errors in general affect the code tracking loop. This is shown analytically and by processing simulated GNSS signals with software receivers.

INTRODUCTION

It is a common understanding within the navigation community that a generic GNSS signal $s(t)$ can be written as

$$s(t) = ac(t)exp\{j2\pi f_{RF}t\} \tag{1}$$

where t is time, a is the signal amplitude, $c(t)$ is the baseband portion of the signal employing the respective modulation scheme like BPSK or BOC and f_{RF} is the nominal radio frequency (RF). A potentially present navigation data message is neglected here. The most common modulation schemes use a real valued function $c(t)$ to represent the baseband signal. The resulting power spectrum $S_c(f)$ of $c(t)$ is consequently symmetric with respect to the zero frequency. Furthermore, the spectrum $S_s(t)$ of $s(t)$ is symmetric with respect to the nominal RF.

A potentially present filter in the transmission or reception chain may slightly distort the spectral symmetry, but the filter design should be in a way to minimize those effects. Therefore we neglect filter effect in the following considerations.

A more general case occurs for signals whose spectrum is not symmetric with respect either to the zero frequency or to the nominal RF frequency. To better understand this case, we first discuss generic properties of a spectrum and the autocorrelation function of a navigation signal.

If $S(f)$ denotes a generic signal power spectrum, then $S(f)$ is per construction real-valued. The correlation function $R(\tau)$ is the Fourier transform of the spectrum, i.e.

$$R(\tau) = \frac{1}{\sqrt{2\pi}} \int_{-\infty}^{\infty} S(f) \exp\{2\pi jf\tau\}df \tag{2}$$

The first derivative of the correlation function at zero code delay is

$$D = \frac{d}{d\tau}R(\tau)|_{\tau=0} = \frac{2\pi j}{\sqrt{2\pi}} \int_{-\infty}^{\infty} fS(f)df \tag{3}$$

The real part $\Re\{D\}$ vanishes as the argument of the integral is real-valued and the imaginary part

$$\Im\{D\} = \sqrt{2\pi} \int_{-\infty}^{\infty} fS(f)df \tag{4}$$

differs from zero if and only if the spectrum is asymmetric. This is because the spectrum is multiplied by the odd function f within the integral, yielding finally contributions to integral only for odd parts of $S(f)$.

Overall we may distinguish three different cases of a GNSS signal spectrum:

- Symmetric
- Asymmetric
- Symmetric, but with respect to a different reference frequency (called shifted in the following text)

They are visualized in Fig. 1, where $f = 0$ denotes either the zero frequency or the nominal center frequency. The case of the shifted signal spectrum (an exemplary offset of $f_{VIC} = 5.115$ MHz is chosen in Fig. 1) shows that each spectrally symmetric signal can be converted in a asymmetric signal by doing the replacement

$$\begin{aligned} f_{RF} &\to f_{RF} - f_{VIC} \\ c(t) &\to c(t) \exp\{j2\pi f_{VIC}t\}. \end{aligned} \tag{5}$$

Shifted GNSS signals are used within the VITAL tracking architecture [2] which is explained and evaluated in the next section of this paper.
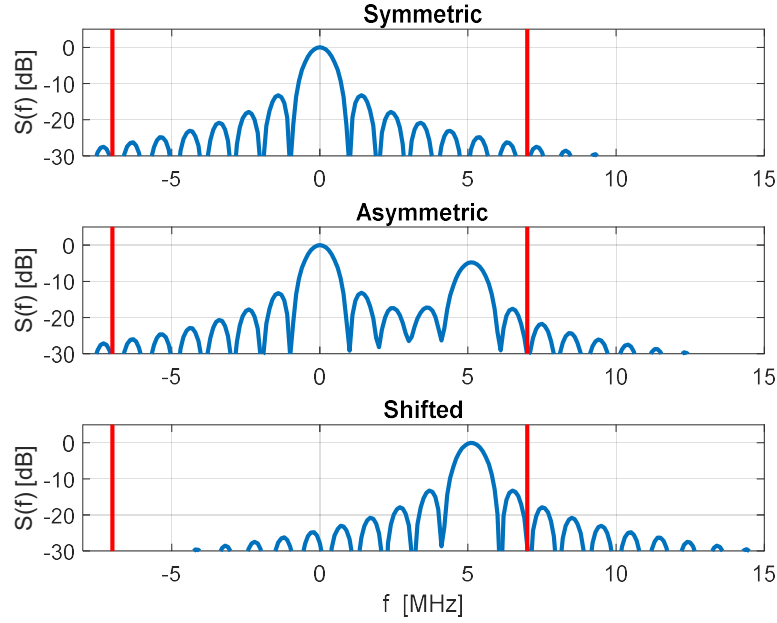
Fig. 1 – Three representative cases of a GNSS signal spectrum; the red lines denote the portion of the signal spectrum considered in the GNSS receiver

Code Tracking Accuracy

We assume an infinite sampling rate within the receiver, neglect the squaring loss and compute the variance of an early-late code discriminator with a discriminator spacing d, a dual-sided signal bandwidth B and a coherent integration time T_{coh}. Furthermore a signal-to-noise ratio C/N_0 is assumed for white noise. The variance of the code discriminator is given (cf. equation (7.122) of [3]) as

$$\sigma^2_{code} = \frac{1}{2C/N_0 T_{coh}} \frac{\int_{-B/2}^{B/2} S_c(f) \sin^2(\pi f d) df}{\left| 2\pi \int_{-B/2}^{B/2} f S_c(f) \sin(\pi f d) df \right|^2}. \tag{6}$$

It should be recalled that $S_c(f)$ has been defined as the power spectral density of the baseband signal $c(t)$ regardless if it is symmetric, asymmetric or shifted. The integration boundaries are chosen independently of $c(t)$ in the sense that for the shifted case, the signal main lobe is not in middle of the integration boundaries. The integration boundaries are denoted as red bars in Fig. 1.

It is well known that the code discriminator variance decreases (and the accuracy increases) if the signal spectrum is located near the edges of the considered signal spectrum. In that case the denominator of (6) increases due to the weighting with f, whereas the nominator has no weighting function. As a consequence, the code tracking accuracy is better for a shifted GNSS signal spectrum than for the symmetric signal spectrum even though both stem from the same GNSS signal source. This is the basis for the correlation peak sharpening used within the VITAL concept.

EXPLOITING SPECTRAL ASYMMETRY – THE VITAL CONCEPT

The VITAL tracking scheme has been introduced and analyzed in [2]. It artificially introduces a variable intermediate frequency (IF) to increase the code tracking accuracy (shifted GNSS signal spectrum). It does this in a clever way and introduces several IF values (and not only one) to properly resolve the correct correlation peak. The correlation function of a spectrally shifted GNSS signal exhibits multiple correlation peaks. By slowly increasing the IF, the code accuracy is gradually increased and at the same time the width of the correlation peak is reduced.

Proof-of-Concept Software Receiver Implementation

The VITAL tracking scheme has been implemented into SoftGNSS v3.0 provided in the CD accompanying the book [1]. The intermediate frequency is f_{IF} = 9.548 MHz, sampled at f_s = 38.192 MHz with a sample width of 8 bits. The variable IF is chosen to vary f_{VIC} = 0 MHz (0 to 10000 ms), 1.1935 MHz (10001 to 20000 ms), 2.387 MHz (20001 to 30000 ms), and 4.774 MHz (30001 to 37000 ms), respectively. Those cases are denoted as VIC(0,1), VIC(1,1), VIC(2,1) and VIC(4,1) respectively. The first number approximately indicates the offset frequency in multiplies of 1 MHz and the second number the code rate of 1.023 MHz. The acronym VIC denotes variable IF code/correlation.

Discussion of Tracking Results and Autocorrelation Function

The code phase errors for VIC(0,1), VIC(1,1), VIC(2,1), and VIC(4,1) are shown in Fig. 2 (a), each lasting about 10 seconds. VIC(0,1) is similar to the conventional normalized early minus late correlation power with ½ chip spacing as shown in Fig. 2 (b). Since the carrier phase errors are calculated on the in-phase and quadrature components of the prompt correlator, both the VITAL and the conventional loop produce similar phase errors as shown in Fig. 2 (c) and (d). The carrier phase errors shown in Fig. 2 (c) are calculated from the prompt correlation. The code phase errors shown in Fig. 2 (a) are calculated from the real components spaced by a ¼ cycle. Fig. 3 shows the correlations for different IF frequencies over samples away from the prompt code phasing (the zero index).

(a) Quadratic fit to early-prompt-late of VIC, spaced by 1/4 cycle, scaled to meet NEMLP

(b) Conventional normalized early minus late correlation power, spaced by ½ chips

(c) atan( ) on prompt correlator of VIC scaled
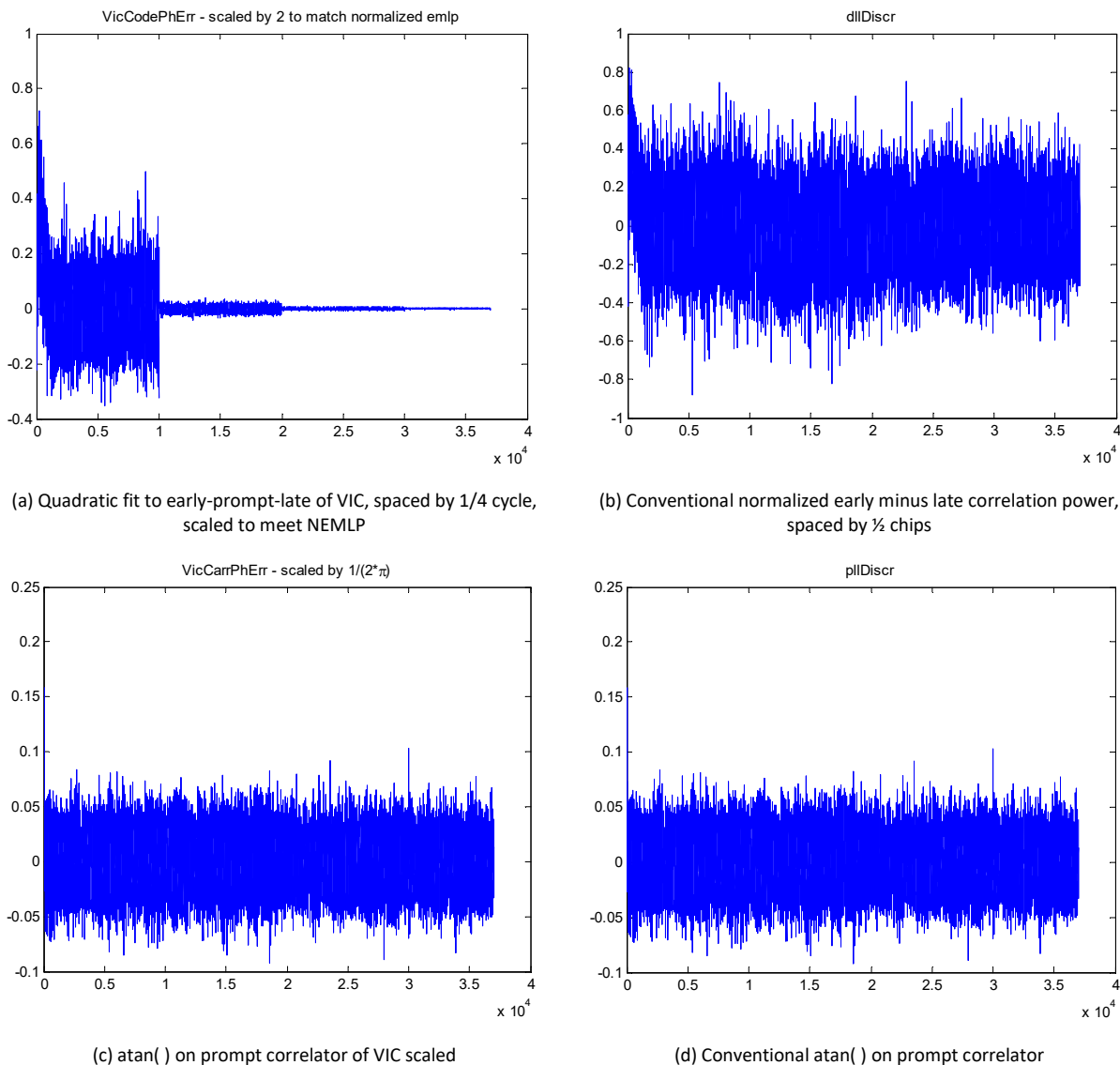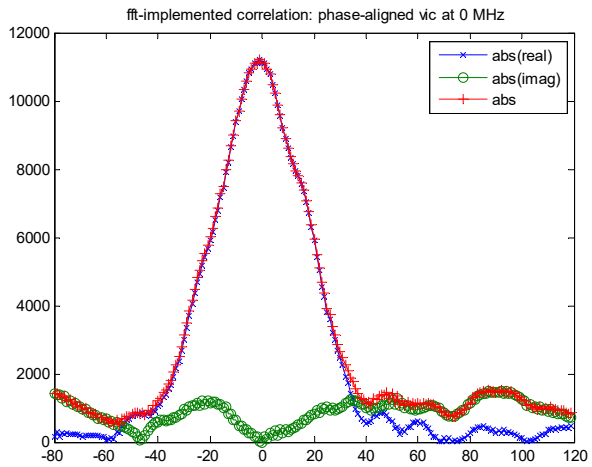
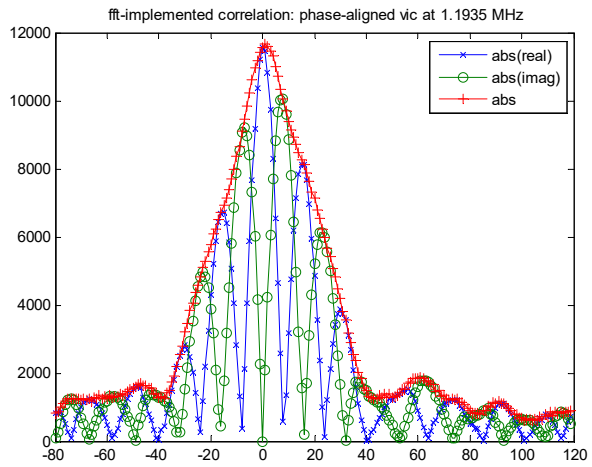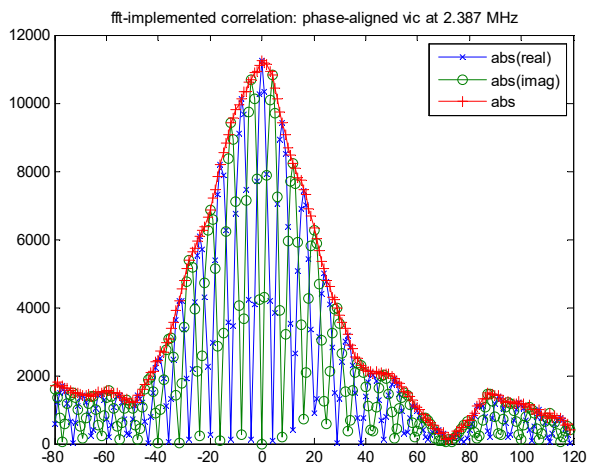(d) Conventional atan( ) on prompt correlator

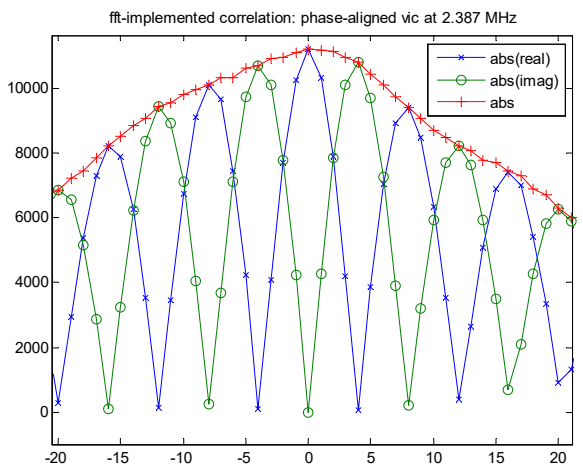**Fig. 2 – Outputs of Code Phase and Carrier Phase Error Discriminators**
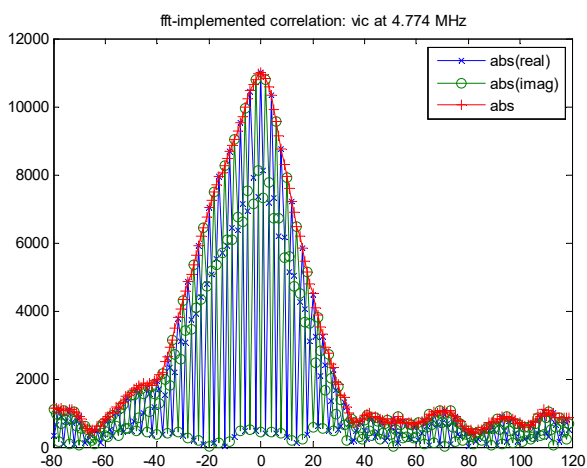
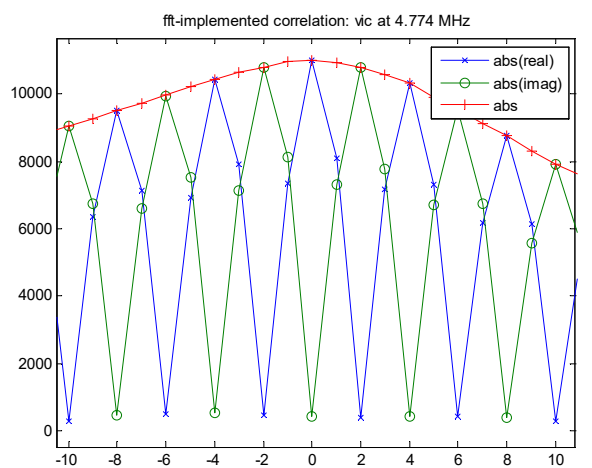(a) VIC(0, 1) ~ Conventional

(b) VIC(1, 1)

(c) VIC(2, 1)

(d) Detail of VIC(2, 1)

(e) VIC(4, 1)

(f) Detail of VIC(4, 1)

Fig. 3 – VIC at Different IF Frequencies

The absolute real (in-phase, blue cross), absolute imaginary (quadrature, green circle), and magnitude (red plus) correlations are plotted. When the carrier phase is aligned, the in-phase component of the prompt has the peak value while the quadrature component has a zero-crossing. This is in accordance with the observation that the imaginary part of the first derivative of the correlation function (3) differs from zero for spectrally asymmetric signals. On contrast, the real part of the first derivative is always zero.

In VIC(1,1), the spacing is 4 samples as shown in Fig. 3 (b). In VIC(2,1), it is 2 samples as shown in Fig. 3 (c) with details in Fig. 3 (d). In VIC(4,1), it is 1 samples as shown in Fig. 3 (e) with details in Fig. 3 (f).

Positioning Results

In the data set provided in [1], there are 8 satellites visible over the first 37 sec, which are processed into the position fixes. The top plot of Fig. 4 shows the variations over time (500 ms per data point) of the north, east, and up components of the position fixes shown in the left plot of Fig. 5 using the conventional tracking and least-square positioning methods provided in [1].

We replaced the conventionally spaced early, prompt, and late correlators (half-chips) with VIC in calculating the code and carrier phase error discriminators used by 1st-order DLL and PLL loop filters (2nd-order loops). The bottom plot of Fig. 4 shows the variations over time of the north, east, and up components of the position fixes shown in the right plot of Fig. 5 using the VITAL method.

The peak to peak errors of the VITAL solution are -4 to 5 m in the east and north components and -6 to 8 m in the up-component while those of the conventional method are -5 to 8 m in the east and north components and -10 to 14 m in the up-component, respectively. Due to scale differences, the blue-shaded area in the top plot of Fig. 4 (excluding the VIC(0, 1) in the first 10 s) represents the east and north components of the VTAL solution in the bottom plot of Fig. 3. The red-shaded area in the top plot of Fig. 4 represents the up-component of the VTAL solution in the bottom plot of Fig. 4. The improvement is 4 m and 10 m in peak to peak errors in the horizontal and vertical components, respectively.

The left plot of Fig. 5 shows the horizontal position errors of the conventional method. In comparison, the horizontal position errors of the VITAL method is shown in the right plot of Fig. 5. Excluding the large errors when VIC(0, 1) is used, which is equivalent to the conventional, the improvement is about ±2 m, consistent with what we have observed from Fig. 4.

In summary, with VITAL - a simple change in what correlations are used to calculate for phase error discriminators - we are able to improve the position errors by about 30% (horizontal) and 50% (vertical).
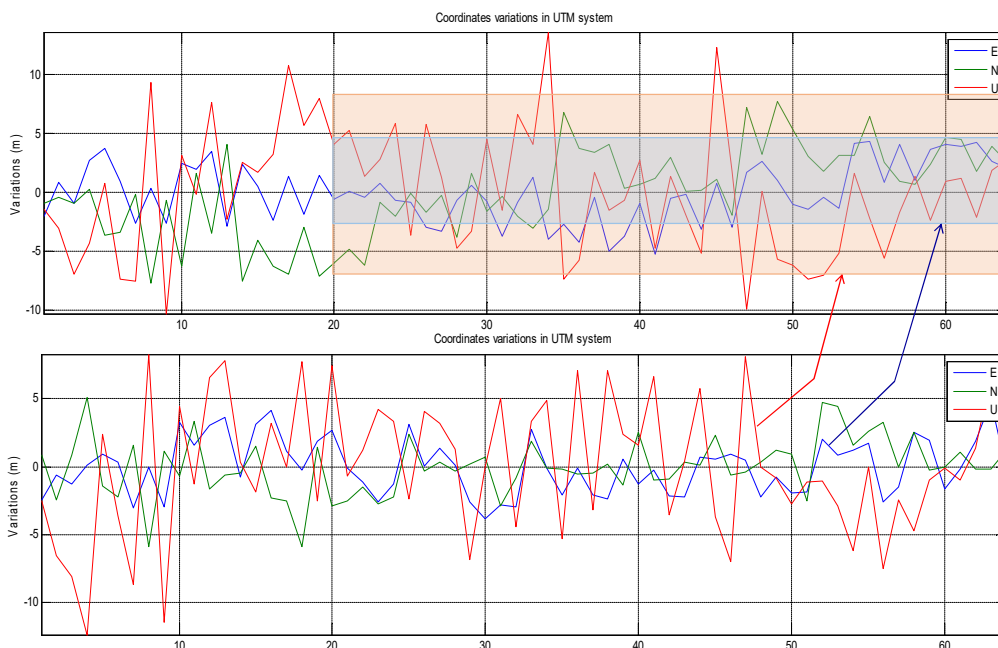

Fig. 4 – Variations in Position Fixes from Conventional Tracking (upper plot) & VITAL Methods (lower plot); 500 ms per data point; the shaded areas in the upper plot represent the variations of the lower plot (red: height, gray: horizontal) for ease of comparison
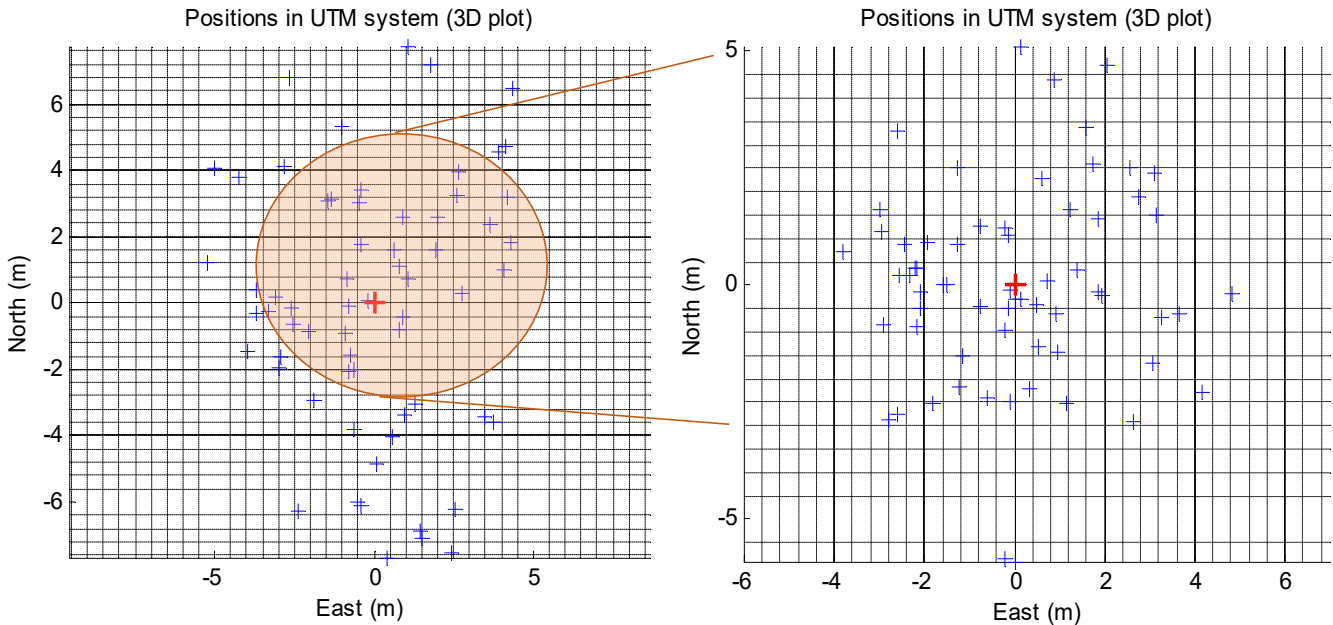
Fig. 5 – Comparison of Position Fixes from Conventional (left) & VITAL Methods (right); the shaded area on the left indicates the variations of the VITAL method for ease of comparison

IN-DEPTH TRACKING ANALYSIS

The previous section showed that the VITAL concept improved the positioning performance to some extent by artificially shifting the IF. The accuracy gain was clearly visible in the code discriminator, but showed up to much less extent in the positioning results. To further investigate this topic, we perform a bit-true simulation of a single GPS C/A code signal, which gives us more detailed options to investigate the tracking performance as the true pseudorange is exactly known. The simulated signal is processed by two software receivers. Based on those results, we propose a theory to explain the observed behavior.

Single Channel Simulation

The following parameters were used to generate a bit-true GPS C/A code signal:

- RF = 1575.42 MHz, IF = 9.548 MHz, Sample rate = 38.192 MHz

- Quantization: 2-bit, dual sided bandwidth (3 dB) = 8.184 MHz

- Simulated C/N0 (before analog-to-digital conversion but after RF filtering): 47 dB-Hz

- Line-of-sight dynamics: 500 m/s with an acceleration of 0.2 m/s^2

- Baseband signal: GPS C/A PRN1, pure pilot, no multipath

Assuming an early/late correlator spacing of 0.107 chip, a coherent integration time of 1 ms, and a DLL bandwidth of 1 Hz, the code noise can be computed to be 0.49 m (1-sigma value). Carrier noise is 0.014 rad (0.43 mm) for a PLL bandwidth of 9 Hz.

Results of First Software Receiver

We first present results from the modified SoftGNSS v3.0 software receiver also used in the previous section. In particular we plot the observed code pseudorange minus the true pseudorange (i.e. the code pseudorange error). It is shown in Fig. 6. We observe that the code ranging accuracy increases from standard tracking to VITAL tracking, but improves only slightly from VIC(1,1) to VIC(4,1). Furthermore, the code accuracy is at the several meter level and thus significantly different from the theoretical prediction. This difference can be well explained by having a look at the SoftGNSS v3.0 implementation of pseudorange formation. The modified SoftGNSS v3.0 coarsely aligns the replica signal to the received signal with the resolution of the sampling rate. It takes the file position in bytes using ftell( ) (number of 8-bit samples) as the coarse time-of-arrival (TOA), which is equivalent to the TOA as calculated by the code phase and code rate from the DLL. Based on this

TOA estimation, the 3 largest correlator values are used to perform a quadratic fit. The position of the maximum of the quadradic fit, representing the code discriminator, is added to the coarse TOA to obtain the estimated pseudorange. It is very important to note that only the real valued correlator values are used (and not the magnitude) in order to exploit the fine structure of the VITAL correlation function (see Fig. 3). At lower VIC [VIC(0,1) and VIC(1,1)], both TOA and code discriminator output change by several samples at 38 Msps. At higher VIC, TOA changes by several samples but code discriminator output only fractional samples (similar to Fig. 2(a)).

As the discriminator noise is one-to-one contained in the code pseudorange (as it is not filtered by the DLL, which only impacts the coarse TOA), it is clear that the code noise is much larger compared the theoretical prediction for a 1 Hz DLL.
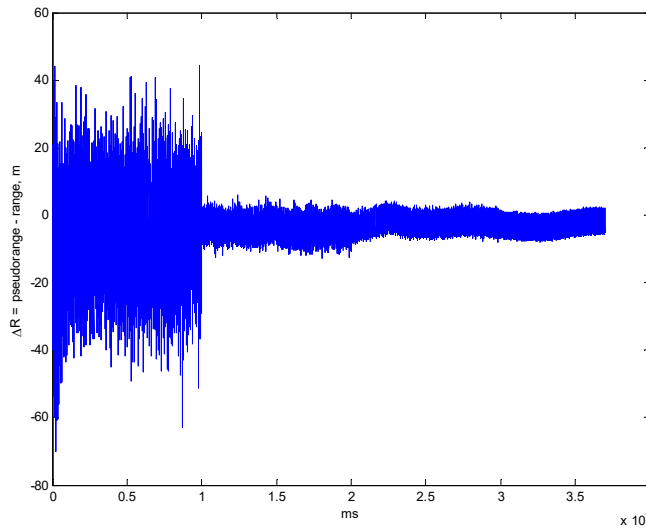

Fig. 6 – Pseudorange error for simulated data using the modified SoftGNSS V3.0 receiver gradually changing the tracking scheme from VIC(0,1) to VIC(~1,1), VIC(~2,1), and VIC(~4,1)

Results of Second Software Receiver

The data was also processed by a second software receiver. This software receiver mimics a classical GNSS receiver and resamples the replica signal based on the code and carrier numerically controlled oscillator (NCO) values and provides code pseudoranges based on the code NCO readings. As code replicas, the GPS C/A baseband signal is multiplied with the VIC carrier as in (5). To compute the code discriminator two steps are performed. First, the instantaneous carrier error is estimated from the prompt correlator. With this estimate, early and late correlators are compensated (i.e. power in the I-channel is maximized for early, prompt and late correlators). Finally, the code discriminator is computed as the normalized early-late difference using only the real part of early and late correlators.

The tracking results are shown in Fig. 7 for standard [= VIC(0,1)] tracking and Fig. 8 for VIC(4,1) tracking.

Similar to the modified SoftGNSS 3.0, we observe a significant reduction of the code discriminator noise for VIC(4,1) tracking. Furthermore, tracking was stable for all considered VIC variants. VIC(1,1) and VIC(2,1) were also tested, but results are not shown here for the sake of simplicity.

For standard tracking the code noise is estimated to be 0.48 m, which confirms well to the theoretical predictions. The bias of around 40 m stems from the simulated RF filter. Also the phase noise confirms well to the theoretical prediction.

However, looking at the code error and phase error for VIC(4,1) tracking, it becomes clear that there is correlation between them. Furthermore, no code accuracy gain is observed for VIC(4,1) tracking compared to standard tracking. The overall code noise is 0.42 m (compared to 0.48 m for standard tracking) but the code noise is highly correlated in time.
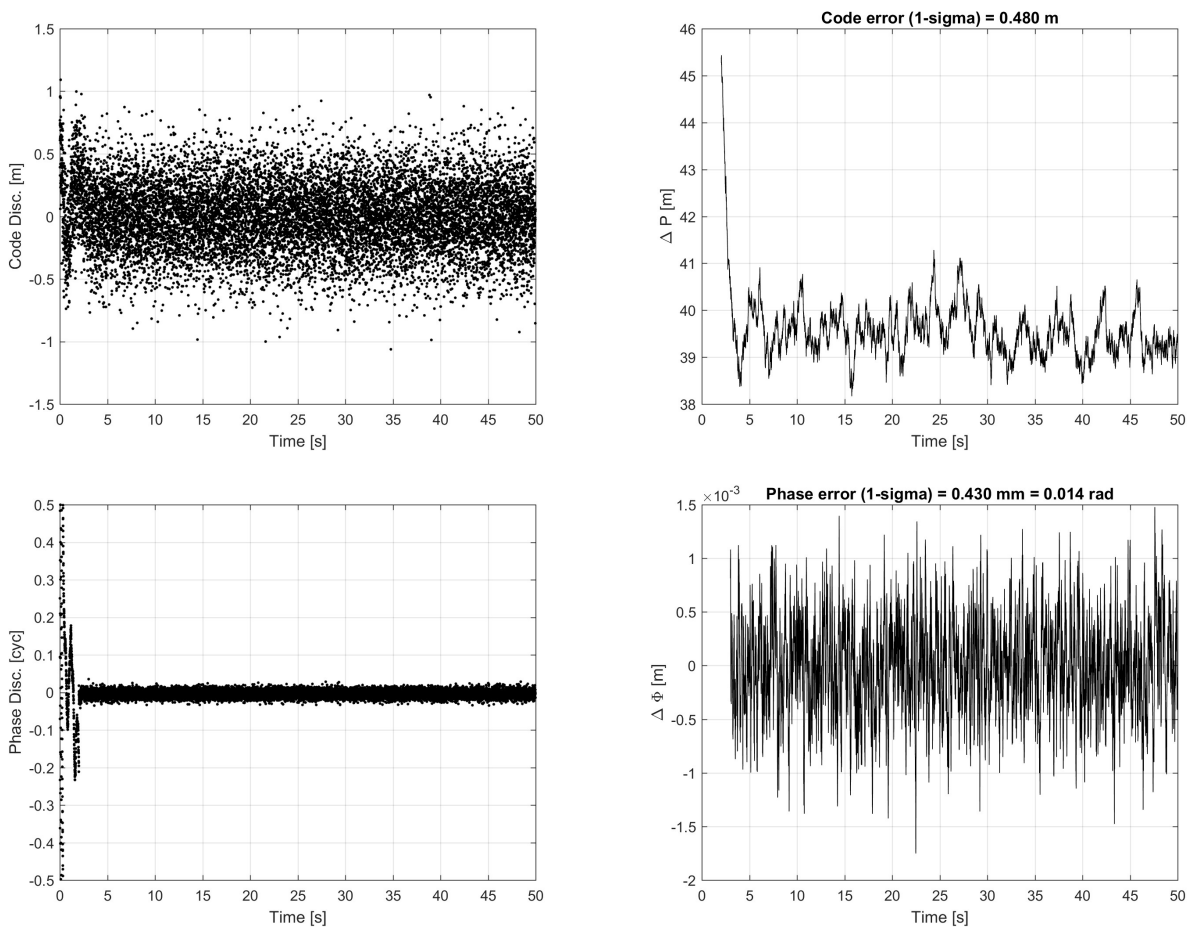
Fig. 7 – Tracking results for simulated data using the second software receiver standard - VIC(0,1) – tracking; upper left: code discriminator, upper right: code pseudorange error, lower left: phase discriminator, lower right: carrier phase error
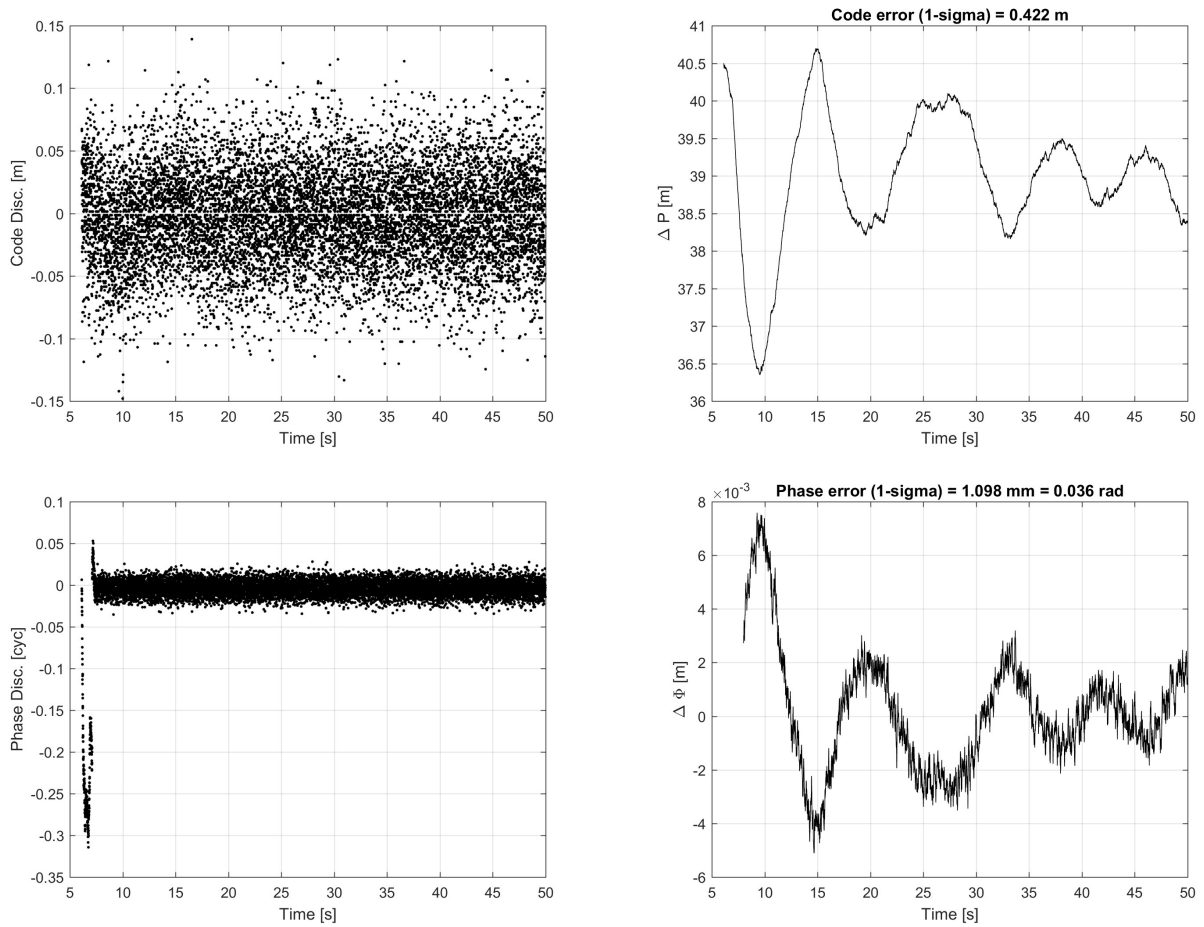
Fig. 8 – Tracking results for simulated data using the second software receiver with VIC(4,1) – tracking; upper left: code discriminator, upper right: code pseudorange error, lower left: phase discriminator, lower right: carrier phase error

Correlated Code Delay and Carrier Phase Estimates

In this section we offer a theoretical explanation to the observed tracking behavior. This explanation is tentative and requires further consolidation.

Whereas spectrally shifted GNSS signals (like the VITAL case discussed before) exhibit an increase in code accuracy, this increase comes at a certain price, which will be outlined in this section. The background for this consideration is an analysis of the signal estimation problem to estimate the four fundamental signal parameters: amplitude a_r, code phase τ, Doppler f_D and carrier phase ϕ, from a batch of received signal samples of duration T_{coh}.

This problem has been analyzed in Section 4.3.2 of [3] by computing the Fisher information matrix (basically the inverse of the covariance matrix of the estimates). To simplify the expressions, the real valued amplitude a_r is now combined with the carrier phase ϕ to obtain the complex valued signal amplitude a as

$$a = a_r e^{j\phi} \tag{7}$$

or

$$a = e^{j\phi} \sqrt{\frac{2C/N_0}{f_s}} \tag{8}$$

if the amplitude is expressed as signal to noise ratio and sampling rate f_s.

Assuming the Doppler to be fixed, the Fisher information matrix I is given according to [3] as

$$I = \begin{pmatrix} I_a & I_{a;\tau} \\ I_{\tau;a} & I_\tau \end{pmatrix} = \frac{f_s T_{coh}}{2} \begin{pmatrix} 1 & aR'(0) \\ aR'(0) & -R''(0)|a|^2 \end{pmatrix}. \tag{9}$$

Off-diagonal elements indicate a correlation between the code phase estimate and the complex valued amplitude estimate.

If Q denotes the covariance matrix between code phase estimate and complex valued amplitude, then

$$Q = I^{-1}. \tag{10}$$

For a fixed real valued signal amplitude, the correlation coefficient between code phase estimate τ and carrier phase estimate ϕ is given by

$$r_{\tau;\phi} = \frac{2Q_{a;\tau}}{j\sqrt{Q_a Q_\tau}}. \tag{11}$$

The derivation of the above equations makes use of the relation between the complex valued amplitude and the carrier phase as outlined in Section 4.3.2.8 of [3].

After computation of the covariance matrix and simplifications we obtain

$$r_{\tau;\phi} = \frac{R'(0)}{\sqrt{R''(0)}} = \frac{\int S_c(f) 2\pi j f \, df}{\sqrt{\int S_c(f)(2\pi j f)^2 df}} = \frac{\int S_c(f) f \, df}{\sqrt{\int S_c(f) f^2 df}}. \tag{12}$$

It is easily seen that for a spectrally symmetric signal $r_{\tau;\phi} = 0$ and the code and carrier estimates are uncorrelated.

In the hypothetical case that the baseband signal consists of a pure carrier located at the frequency f_x, then the spectrum consists of a Dirac delta function $S(f) = \delta(f - f_x)$ and $r_{\tau;\phi} = 1$. In that case code and carrier estimates are totally correlated, which is expected as both (code and carrier) have an indistinguishable waveform.

For the general asymmetric case, a certain amount of correlation is expected. Uncorrelated measurements can always be achieved even for a spectrally asymmetric signal source, if the nominal RF is redefined to match the "center of mass" of the signal spectrum. This can be expressed as

$$S(f) \rightarrow S(f - f_{COM}) \tag{13}$$

with

$$f_{COM} = \frac{\int S(f) f \, df}{\int S(f) df}. \tag{14}$$

For spectrally symmetric signals, the center of mass RF equals the nominal RF.

Expected Impact on Tracking Performance

The impact of the correlation is that a carrier tracking error will spill over into a code tracking error. As carrier tracking errors are more likely to occur than code tracking errors, the code carrier correlation will negatively influence the code tracking stability. For example a cycle slip on the carrier tracking loop, will cause a code bias as long as the carrier tracking loop does not fully recover from the cycle slip. Furthermore, this correlation may explain the tracking behavior shown in Fig. 8 for VIC(4,1) tracking; code and carrier tracking errors may compensate themselves finally resulting in a similar accuracy as for standard tracking.

CONCLUSIONS

Spectral asymmetric signals potentially exhibit a nominally higher code tracking accuracy than spectrally symmetric signals due to the increased Gabor bandwidth. Spectral asymmetric signals can either be directly generated by the transmitter or the GNSS receiver can artificially create them be redefining the center frequency. The VITAL concept exploits this and thus targets a gradual incorporation of carrier accuracy into code tracking. In case uncorrelated code and carrier estimates are required even for asymmetric signals per transmission, a redefinition of the nominal RF to the center of mass RF can achieve this target.

Two different software receivers were used to investigate the VITAL scheme with real and simulated signals. Whereas we could prove that the VITAL scheme allows stable tracking even for real-world GPS C/A signal and provides accuracy gain, a

more detailed analysis shows some inconsistencies and partly correlations between code and carrier estimates. Whereas the theory of asymmetric signals can be used to explain part of the observed phenomena, further research is required to fully understand the tracking process and to eventually reach the full increased code tracking accuracy due the higher Gabor bandwidth.

REFERENCES

[1]   Borre, K., Akos, D.M., Bertelsen, N., Rinder, P., Jensen, S.H.: "A Software-Defined GPS and Galileo Receiver: A Single-Frequency Approach" by Birkhäuser Basel, 2007.

[2]   Yang, Chun, "Sharpen the Correlation Peak: A Novel GNSS Receiver Architecture with Variable IF Correlation", *NAVIGATION, Journal of The Institute of Navigation*, Vol. 63, No. 3, Fall 2016, pp. 249-265.

[3]   Pany, Thomas. *Navigation signal processing for GNSS software receivers.* Artech House, 2010.

[4]   M. Paonni, J.T. Curran, M. Bavaro, and J. Fortuny-Guasch, "GNSS Meta-Signals: Coherent Composite Processing of Multiple GNSS Signals," ION-GNSS+ 2014, Sept. 2014.

[5]   D. Borio, "Double Phase Estimator: a New Unambiguous BOC Tracking Algorithm," IET Radar, Sonar and Navigation, 8(7), 729-741, 2014.